Am J Cancer Res 2018;8(3):387-404
www.ajcr.us /ISSN:2156-6976/ajcr0070155

Original Article

BCL7B, a predictor of poor prognosis of pancreatic cancers, promotes cell motility and invasion by influencing CREB signaling

Keisuke Taniuchi[1,2], Mutsuo Furihata[3], Seiji Naganuma[3], Ken Dabanaka[4], Kazuhiro Hanazaki[4], Toshiji Saibara[1,2]

Departments of [1]Gastroenterology and Hepatology, [2]Endoscopic Diagnostics and Therapeutics, [3]Pathology, [4]Surgery, Kochi Medical School, Kochi University, Nankoku, Kochi 783-8505, Japan

Received December 1, 2017; Accepted December 12, 2017; Epub March 1, 2018; Published March 15, 2018

Abstract: The functions of B-cell CLL/lymphoma 7B (BCL7B) are unknown and the protein lacks any known functional domains. The aim of this study was to investigate the role of BCL7B in the motility and invasiveness of pancreatic cancer cells. Immunohistochemistry was performed to determine whether high BCL7B expression in human pancreatic cancer tissues is correlated with poor prognosis. High BCL7B expression was an independent predictor of worse overall survival of pancreatic cancer patients. Immunocytochemistry showed that BCL7B was accumulated in cell protrusions of migrating pancreatic cancer cells. Knockdown of BCL7B inhibited the motility and invasiveness of pancreatic cancer cells through a decrease in cell protrusions. Phosphoprotein array analysis was performed to determine BCL7B-associated intracellular signaling pathways. Suppression of *BCL7B* increased phosphorylated CREB expression in pancreatic cancer cells, and knockdown of *CREB* promoted the motility and invasiveness by increasing cell protrusions. The combined data suggest that BCL7B promotes pancreatic cancer cell motility and invasion through a signaling pathway that involves dephosphorylation of CREB.

Keywords: BCL7B, pancreatic cancer, cell invasion, CREB, actin-cytoskeleton

Introduction

The B-cell CLL/lymphoma 7 (BCL7) family includes three members, BCL7A, BCL7B, and BCL7C. The family was discovered through the involvement of the *BCL7A* gene in a complex translocation seen in a Burkitt lymphoma cell line [1]. The cloning of chromosomal translocations from haematologic malignancies has facilitated the identification of several gene families of importance in the control of normal cell differentiation, proliferation and cell death [2]. Although this phenomenon points to potentially important roles of the BCL7 family, particularly BCL7A, in the regulation of cell growth, chromosomal rearrangements affecting *BCL7B* or *BCL7C* have not been detected in hematologic malignancies [3]. *BCL7B* belongs to a family of highly conserved genes involved in early embryonic development; *BCL7B* is located in a region at 7q11.23 which is consistently deleted in the Williams-Beuren contiguous gene deletion syndrome [3]. Hemizygous loss of 7q11.23, and the concomitant reduced expression of *BCL7B*, has been reported in pilocytic astrocytomas [4]. Despite these potentially important links to disease, the cellular roles of the *BCL7* family are largely unknown, and the proteins lack any known functional domains [5].

CREB belongs to the leucine zipper class of transcription factors [6, 7]. Pathologically, CREB promotes hepatocellular carcinoma progression by promoting angiogenesis and resistance to apoptosis [8]. Phosphorylated CREB interacts with diverse transcriptional co-activators, including the histone acetyltransferases and CREB-binding protein (CBP/p300), thereby increasing CREB's transcriptional activity [9, 10]. CREB activates transcription in response to cAMP, intracellular Ca^{2+}, various growth factors (e.g. nerve growth factor, fibroblast growth factor and the insulin growth factor 1), as well as cytokines, including IL-4, IL-10, IL-13 and trans-

forming growth factor-β [11, 12]. CREB activity might also be controlled by its subcellular localization [13]. The underlying molecular mechanisms driving CREB overexpression and activation in tumors have not yet been elucidated in detail [14]. In some cases, CREB is considered to be an oncogenic transcription factor because it is overexpressed and/or constitutively phosphorylated in several human cancers, and induces a cell growth and antiapoptotic survival signal [15]. The functions of CREB in PDAC remain unknown.

Here, we show that the overexpression of BCL7B in pancreatic cancer tissue is significantly correlated with overall survival, and BCL7B contributes to the formation of additional membrane protrusions by decreasing CREB phosphorylation, resulting in increased motility and invasiveness of PDAC cells.

Material and methods

Antibodies

Anti-BCL7B antibody (H00009275) was purchased from Abnova (Taipei City, Taiwan). The JLA20 anti-actin antibody (MABT219) was purchased from Merck Millipore (Temecula, CA). Anti-myc (sc-789) antibody was purchased from Santa Cruz Biotechnology (Santa Cruz, CA). Anti-BCL7A antibody (C20948) was purchased from Assay Biotechnology Company (Sunnyvale, CA). Anti-CREB antibody (A301-669A) was purchased from Bethyl Laboratories (Montgomery, TX).

Primary human PDAC samples

Tumor tissues were obtained from 102 patients who underwent surgical treatment for PDAC and received surgical resection during 1999-2014 at the Departments of Surgery, Kochi Medical School Hospital (Nankoku, Japan) and Matsuyama Shimin Hospital (Matsuyama, Japan), as published previously [16]. All patients had clinical records and none of them received chemotherapy or radiation therapy before surgery. Of these patients, 83 received adjuvant chemotherapy with gemcitabine or S-1, or chemoradiation therapy after resection of PDAC. Tumors were classified according to the classification of pancreatic carcinoma of the Japan Pancreas Society [17] and UICC TNM classification [18]. The study was approved by the ethical review board of Kochi Medical School and Matsuyama Shimin Hospital prior to patient recruitment. Written informed consent was acquired from each patient prior to initiation.

Immunohistochemical staining

Immunohistochemistry was carried out, as published previously [16]. Tissue sections from normal pancreas, brain, lung, liver and kidney were purchased from Biochain (Hayward, CA).

Evaluation of BCL7B staining

Staining was evaluated by two independent observers (SN and MF) who were blinded to clinical and outcome data. BCL7B expression levels were classified semi-quantitatively based on the total combined scores of positive-staining tumor cell percentage (1, < 50% reacting cells; 2, 50-80% reacting cells; 3, > 80%) and staining intensity (1, weaker than the intensity of surface staining in the islet of Langerhans; 2, equal to the intensity of the islet of Langerhans; 3, stronger than the intensity of the islet of Langerhans). A total immunohistochemical score was calculated by summing the percentage score and the intensity score. BCL7B expression was classified into two groups based on total score (low group, 2-3; high group, 4-6) with reference to a previous report [16, 19].

Cell culture

The human PDAC cell line S2-013, a subline of SUIT-2, was obtained from Dr. T. Iwamura (Miyazaki Medical College, Miyazaki, Japan) [20]. The human PDAC cell line, PANC-1 [21] was purchased from the American Type Culture Collection (Manassas, VA). HPNE immortalized normal pancreatic epithelial cells were a kind gift from Dr. Michel Ouellette (University of Nebraska Medical Center, NE) [22]. All cells were grown in Dulbecco's modified Eagle's medium (DMEM; Gibco-BRL, Carlsbad, CA) supplemented with 10% heat-inactivated fetal calf serum (FCS) at 37°C in a humidified atmosphere saturated with 5% CO_2.

Confocal immunofluorescence microscopy

Immunocytochemistry was carried out, as published previously [23]. Briefly, coverslips were coated with 10 μg/mL fibronectin (Sigma-Aldrich, St. Louis, MO) for 1 h at room tempera-

ture. S2-013 cells were seeded on fibronectin-coated glass coverslips, incubated for 5 h; and then fixed with 4% paraformaldehyde and permeabilized with 0.1% Triton X-100. Blocking solution (3% BSA/PBS) was added, followed by incubation with the primary antibody for 1 h. After washing, Alexa488-, Alexa594-, or Alexa647-conjugated secondary antibody (Molecular Probes, Carlsbad, CA) was applied. In some experiments, a commercial antibody-labeling technology (Zenon; Life Technologies, Carlsbad, CA) was used according to the manufacturer's instructions to conjugate green or red fluorophores to primary antibodies. Each specimen was visualized using a Zeiss LSM 510 META microscope (Carl Zeiss, Gottingen, Germany).

PDAC cells that formed cell protrusions, in which peripheral actin structures were accumulated, were counted by two blinded individuals (KD and KH). Four independent visual fields were counted via microscopic observation to count the number of cells that formed cell protrusions. Data are derived from three independent experiments.

siRNA treatment

A single mixture with four different siRNA oligonucleotides targeting *BCL7B* or *CREB* was purchased from Qiagen (FlexiTube GeneSolution GS9275 and GS1385, respectively; Valencia, CA) and a single mixture with four different scrambled negative control siRNA oligonucleotides was obtained from Santa Cruz (37007). One day prior to transfection, S2-013 and PANC-1 cells that expressed BCL7B and CREB were seeded to ensure that density was at 40-50% confluence at the time of transfection. The cells were transfected with 80 pmols of each siRNA mixture in siRNA transfection reagent (Qiagen) following the manufacturer's instructions. After incubation for 48 h, the cells were harvested for functional studies or molecular analyses as described below.

Immunoblot analysis of cell lysates

Each cell pellet was extracted using lysis buffer [Tris-HCl (pH 7.4), sodium dodecyl sulfate (SDS), mercaptoethanol and glycerol]. The cell extracts were boiled for 5 min in loading buffer and then an equal amount of cell extract was analyzed by SDS-poly acrylamide gel electrophoresis (PAGE) and western blotting. Primary antibodies were diluted according to the manufacturer's instructions and incubated overnight at 4°C. Subsequently, horseradish peroxidase-linked secondary antibodies were added at a dilution of 1:5,000 and incubated at room temperature for 1 h. The membranes were washed with PBS and the immunoreactive bands were visualized using the ECL Plus kit according to the manufacturer's instructions.

In vitro growth rate by MTT assay

Cells were each seeded at a concentration of 5×10^4 cells per well using 12-well plates. The viability of cells was evaluated by 3-(4,5-dimethylthiazol-2-yl)-2,5-diphenyltetrazolium bromide (MTT) assay according to the manufacturer's instructions. Briefly, cell counting kit-8 solution (Dojindo, Kumamoto, Japan) was added to each well at a concentration of 1/10 volume, and the plates were incubated at 37°C for an additional 3 h. Absorbance was then measured at 490 nm, and at 630 nm as a reference, with a Microplate Reader 550 (Bio-Rad, Hercules, CA).

Trans-well motility assay

Cells (3.0×10^4) were plated in the upper chamber of BD BioCoat Control Culture Inserts (24-well plates, 8-μm pore size; Becton Dickinson, San Jose, CA). Serum-free culture medium was added to each upper chamber, and medium containing 5% FCS was added to the lower chamber. After a 12-h incubation, four independent visual fields were examined microscopically to count the number of cells that had moved to the lower chamber.

Matrigel invasion assay

A two-chamber invasion assay was used to assess cell invasion (24-well plates, 8-μm pore size membrane coated with a layer of Matrigel extracellular matrix proteins; Becton Dickinson). Cells (4.0×10^4) suspended in serum-free medium were seeded into the upper chamber and allowed to invade towards a 5% FCS chemoattractant in the lower chamber. After a 20-h incubation, four independent visual fields were examined microscopically to count the number of cells that had moved to the lower chamber.

BCL7B- and CREB-rescue construct

Reverse transcription-PCR (RT-PCR) was used to amplify the entire coding sequence of *BCL7B*

Table 1. Summary of characteristics in 102 patients of pancreatic cancer

Characteristics	Percentage (%)		Charasteristics	Percentage (%)	
Age at surgery			Distant metastasis*		
40-50	3.9	[n = 4]	M0	96.1	[n = 98]
50-60	16.7	[n = 17]	M1	3.9	[n = 4]
60-70	31.4	[n = 32]	Histology†		
70-80	40.2	[n = 41]	PanIN	2.0	[n = 2]
> 80	7.8	[n = 8]	Well	30.4	[n = 31]
Gender			Moderate	55.8	[n = 57]
Male	54.9	[n = 56]	Poor	11.8	[n = 12]
Female	45.1	[n = 46]	Venous invasion†		
Stage*			v0	55.4	[n = 57]
0	2.0	[n = 2]	v1	30.7	[n = 31]
IA	3.9	[n = 4]	v2	10.9	[n = 11]
IB	7.8	[n = 8]	v3	3.0	[n = 3]
IIA	31.4	[n = 32]	Lymphatic invasion†		
IIB	48.1	[n = 49]	ly0	42.6	[n = 43]
III	2.9	[n = 3]	ly1	33.6	[n = 34]
IV	3.9	[n = 4]	ly2	19.9	[n = 21]
Primary tumor*			ly3	3.9	[n = 4]
Tis	2.0	[n = 2]	BCL7B expression		
T1	5.9	[n = 6]	Low	72.5	[n = 74]
T2	14.6	[n = 15]	High	27.5	[n = 28]
T3	75.5	[n = 77]			
T4	2.0	[n = 2]			
Regional lymph nodes*					
N0	46.1	[n = 47]			
N1	53.9	[n = 55]			

*, Classified according to the classification of International Union against Cancer; †, Classified according to the classification of pancreatic cancer of Japan Pancreas Society; PanIN, pancreatic intraepithelial neoplasia.

and *CREB* mRNA. The resultant PCR product was inserted into a pCMV6-Entry vector (Origene Technologies, Rockville, MD) bearing a C-terminal myc-DDK-tag. X-tremeGENE HP DNA Transfection Reagent (Roche, Penzberg, Germany) was used to transiently transfect target cells with the BCL7B-rescue construct and the CREB-rescue construct.

Determination of patterns of protein phosphorylation

Relative phosphorylation levels of 38 selected proteins in scrambled control-siRNA transfected S2-013 cells and *BCL7B*-siRNA transfected S2-013 cells were obtained by profiling 46 specific phosphorylation sites using the Proteome Profiler Human Phospho-Kinase Array Kit ARY003 from R&D Systems (Minneapolis, MN), as published previously [24].

Statistical analysis

For the Immunohistochemical analysis, we performed statistical analysis using R (version 3.3.3; The R Foundation, Wien, Austria), as published previously [16]. Fisher's exact test was used to assess the association between BCL7B expression levels and clinicopathological parameters. The following parameters were examined: age, sex, and the TNM classification or pathological stage, based on the Japan Pancreas Society [17] and UICC [18] scoring systems. Overall survival time was measured from the date of surgery to the date of death due to any cause, or last clinical follow-up as determined by review of electronic medical records. Survival curves were plotted using the Kaplan-Meier method and were compared using the log-rank test (Mantel-Cox). Survival rates are expressed as the median value and interquartile range (IQR). Independent factors for overall survival including age, sex and pathological stage were assessed with Cox proportional hazards regression analysis. The relative hazard for each patient was calculated from coefficients determined by Cox regression. For the *in vitro* experiments, StatFlex software (Ver6; YUMIT, Osaka, Japan) and SAS software (Ver 9.1.3; SAS Institute, Cary, NC) were used for statistical analysis. Student's *t*-test was used for the comparison of continuous variables. *P* values < 0.05 were considered to be statistically significant, and all tests were two-tailed.

Results

BCL7B expression in human PDAC tissues

In the surgical specimens from 102 patients with PDAC, expression levels of BCL7B were

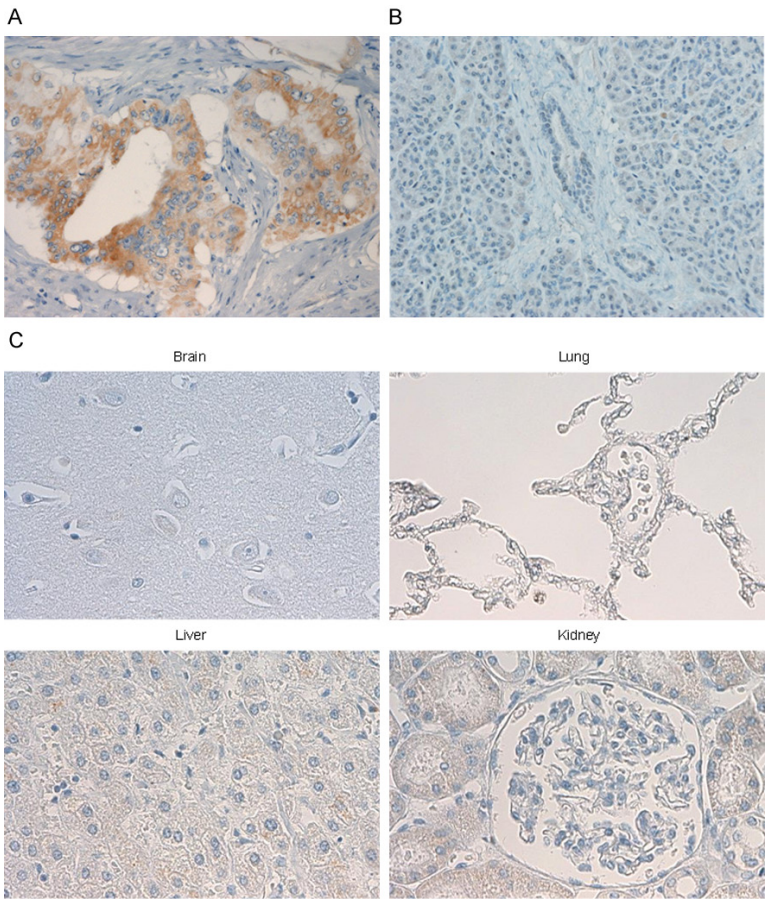

Figure 1. Immunohistochemistry with anti-BCL7B antibody. A. Immunohistochemical staining of PDAC tissues using anti-BCL7B antibody. Magnifications: × 200. B. Expression of BCL7B in normal pancreas. Magnifications: × 200. C. Representative BCL7B staining of normal brain, lung, liver and kidney. Magnification: × 200.

evaluable in all 102 cases, and the specimens were classified into low-expressing (72.5%) and high-expressing (27.5%) BCL7B groups (**Table 1**). BCL7B was localized in the cytoplasm of cell bodies in PDAC cells (**Figure 1A**). BCL7B immunoreactivity was not seen in normal pancreatic ducts (**Figure 1B**). Normal brain, lung, liver and kidney were not obviously stained with the anti-BCL7B antibody (**Figure 1C**).

Association between BCL7B expression, and clinicopathological characteristics, and survival

The associations between BCL7B expression and clinicopathological factors are shown in **Table 2**. There was no significant correlation found between overall expression score and the clinicopathological features examined.

Next, we examined the correlation between BCL7B expression and PDAC patient prognosis. The follow-up period for the 102 PDAC survivors ranged from 18 to 192 months (median, 64.0 mo). Kaplan-Meier survival analysis showed that the overall survival time for patients with high BCL7B expression was significantly shorter than that of patients with low BCL7B expression ($P < 0.001$) (**Figure 2A** and **2B**). Furthermore, univariate and multivariate analyses were used to confirm the independent prognostic significance of BCL7B in PDAC (**Table 3**). Univariate and multivariate analyses revealed that stage III and IV and high BCL7B expression were independent prognostic factors for worse patient survival. These results suggested that BCL7B participated in PDAC progression.

Subcellular localization of BCL7B in PDAC cells grown on fibronectin

Immunocytochemistry was used to determine the subcellular localization of BCL7B in two types of cultured PDAC cell lines; moderately differentiated (S2-013) [20] and poorly differentiated (PANC-1) [21]. Fibronectin induces the formation of membrane protrusions at the leading edge of PDAC cells [23, 25]. There were fewer membrane protrusions formed by S2-013 and Panc-1 cells when the cells were cultured without fibronectin than when the cells are grown on fibronectin [23]. In S2-013 and PANC-1 cells cultured on fibronectin, BCL7B was mainly present in the cytoplasm of cell bodies, and BCL7B was also localized in the nucleus and membrane protrusions, each of which had many peripheral actin structures (**Figure 3A**). In addition, it was noted that BCL7B, which accumulates in membrane protrusions containing many peripheral actin structures, accumulated in abundance in the S2-013 and PANC-1 cells

Table 2. Correlation between BCL7B expression and clinicopathological parameters

	BCL7B expression				*P*
	Low		High		
	Percentage (%)				
Stage*					0.572
0	1.4	[n = 1]	3.6	[n = 1]	
IA	4.0	[n = 3]	3.6	[n = 1]	
IB	9.5	[n = 7]	3.6	[n = 1]	
IIA	31.1	[n = 23]	32.1	[n = 9]	
IIB	48.6	[n = 36]	50.0	[n = 14]	
III	2.7	[n = 2]	0	[n = 0]	
IV	2.7	[n = 2]	7.1	[n = 2]	
Primary tumor*					0.258
Tis	1.4	[n = 1]	3.6	[n = 1]	
T1	6.7	[n = 5]	3.6	[n = 1]	
T2	17.6	[n = 13]	7.1	[n = 2]	
T3	71.6	[n = 53]	85.7	[n = 24]	
T4	2.7	[n = 2]	0	[n = 0]	
Regional lymph nodes*					1
N0	45.9	[n = 34]	46.4	[n = 13]	
N1	54.1	[n = 40]	53.6	[n = 15]	
Distant metastasis*					0.302
M0	97.3	[n = 72]	92.9	[n = 26]	
M1	2.7	[n = 2]	7.1	[n = 2]	
Histology†					0.774
PanIN	1.4	[n = 1]	3.6	[n = 1]	
Well	29.7	[n = 22]	32.1	[n = 9]	
Moderate	58.1	[n = 43]	50.0	[n = 14]	
Poor	10.8	[n = 8]	14.3	[n = 4]	
Venous invasion†					1
v0 + v1	86.5	[n = 64]	85.7	[n = 24]	
V2 + v3	13.5	[n = 10]	14.3	[n = 4]	
Lymphatic invasion†					0.798
ly0 + ly1	74.3	[n = 55]	78.6	[n = 22]	
ly2 + ly3	25.7	[n = 19]	21.4	[n = 6]	

*, Classified according to the classification of International Union against Cancer; †, Classified according to the classification of pancreatic cancer of Japan Pancreas Society; PanIN, pancreatic intraepithelial neoplasia.

cultured on fibronectin compared with the corresponding cells that were not cultured on fibronectin (**Figure 3A**). Z stack panels showed that S2-013 cells grown on fibronectin exhibited intracellular expression of BCL7B in membrane protrusions (**Figure 3B**). BCL7B was weakly expressed in the normal pancreatic ductal HPNE cells [22] cultured on fibronectin and in HPNE cells not cultured on fibronectin (**Figure 3C**).

Localization of BCL7B in cell protrusions

To quantitate the subcellular distribution of BCL7B in S2-013 and PANC-1 cultured with or without fibronectin, cell lysates were fractionated into detergent-soluble and -insoluble (cytoskeletal) fractions. The amounts of BCL7B and actin in the insoluble fraction increased in response to culture on fibronectin (**Figure 4A**), which indicates that BCL7B translocated from cytosol to the actin cytoskeletal fraction following culture on fibronectin.

To determine whether alteration of actin cytoskeleton dynamics could directly affect the subcellular distribution of BCL7B, we treated S2-013 and PANC-1 cells with the actin depolymerising agent, Cytochalasin D. There were fewer peripheral actin structures in fibronectin-stimulated S2-013 and PANC-1 cells exposed to 100 μM Cytochalasin D for 12 h than in fibronectin-stimulated non-treated cells and BCL7B was localized in the cytoplasm in the treated cells (**Figure 4B**). BCL7B was localized in cell protrusions of fibronectin-stimulated non-treated S2-013 and PANC-1 cells (**Figure 4B**).

Roles of BCL7B in cell motility and invasion of PDAC cells

To determine whether BCL7B was involved in the motility and invasiveness of PDAC cells, BCL7B expression in S2-013 and PANC-1 cells was transiently suppressed by *BCL7B*-specific small interfering RNA (siRNA) (**Figure 5A**). The expression of another BCL7 family member, BCL7A, did not change in response to *BCL7B*-siRNA-transfection (**Figure 5A**). Silencing of BCL7B in S2-013 and PANC-1 cells did not affect cell growth in an *in vitro* MTT assay (**Figure 5B**). Silencing of BCL7B significantly reduced cell motility in these PDAC cell lines (**Figure 5C**). Cellular invasive potential was similarly assayed using Matrigel-coated Boyden chambers, and cell invasion was significantly reduced by silencing of BCL7B in S2-013 and PANC-1 cells (**Figure 5D**). A BCL7B-rescue

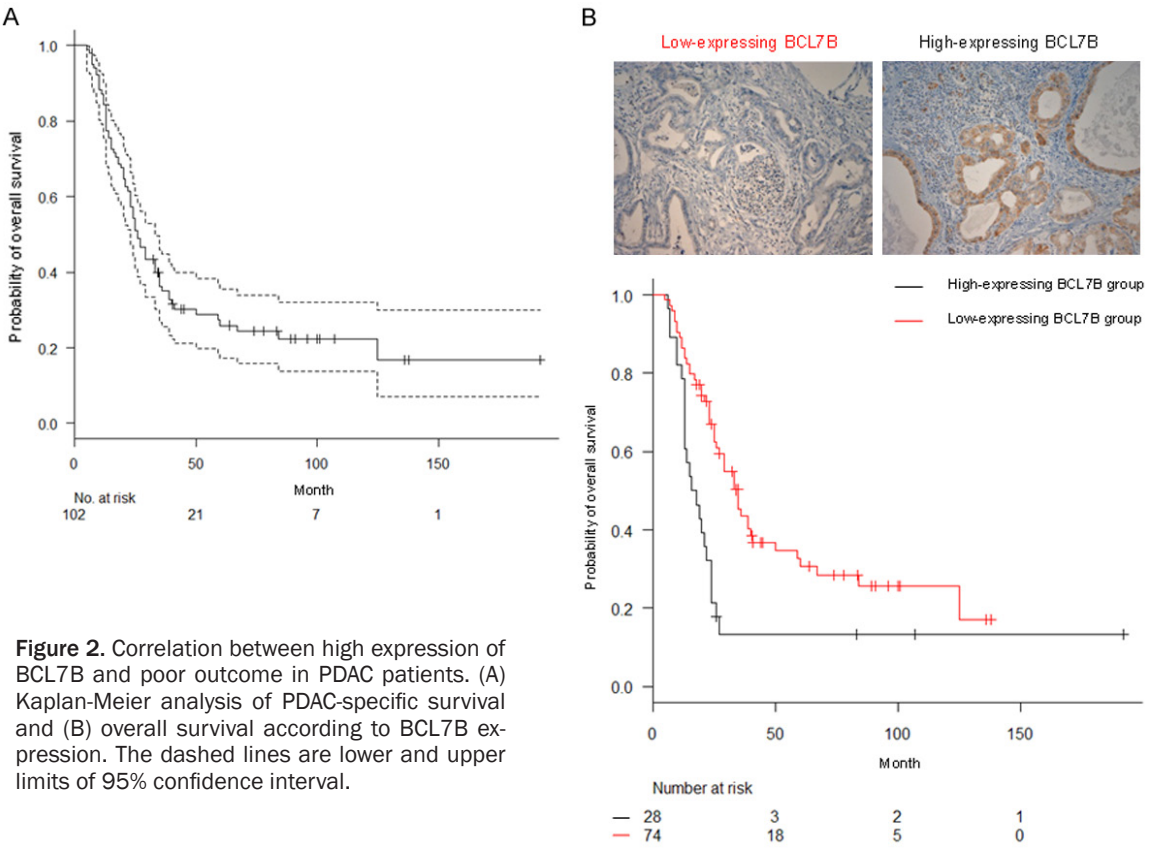

Figure 2. Correlation between high expression of BCL7B and poor outcome in PDAC patients. (A) Kaplan-Meier analysis of PDAC-specific survival and (B) overall survival according to BCL7B expression. The dashed lines are lower and upper limits of 95% confidence interval.

Table 3. Univariate and multivariate analysis of prognostic factors for overall survival

	Overall survival			
	Univariate		Multivariate	
	HR (95% CI)	*P*	HR (95% CI)	*P*
Stage*				
0 + IA + IB	1.0 (reference)		1.0 (reference)	
IIA	1.159 (0.714-1.881)	0.549	6.547 (2.183-19.64)	8.009e-04
IIB	1.356 (0.854-2.151)	0.196	6.961 (2.374-20.41)	4.078e-04
III + IV	3.035 (1.301-7.081)	0.010	16.61 (4.419-62.42)	3.185e-05
Age	1.021 (0.995-1.048)	0.110	1.016 (0.989-1.043)	0.233
Gender	1.107 (0.696-1.761)	0.666	1.196 (0.747-1.913)	0.455
BCL7B expression	0.440 (0.267-0.726)	0.001	0.343 (0.195-0.603)	1.960e-04
Diameter of primary tumor	1.338 (1.176-1.524)	1.045e-05		
Histology†	1.383 (0.846-2.261)	0.1965		
Lymphatic invasion† (ly0 + ly1 or ly2 + ly3)	1.269 (0.751-2.145)	0.3733		
Venous invasion† (v0 + v1 or v2 + v3)	1.928 (1.034-3.593)	0.0388		
Intrapancreatic nerve invasion† (n0 + n1 or n2 + n3)	1.500 (0.947-2.377)	0.0839		

*, Classified according to the classification of International Union against Cancer; †, Classified according to the classification of pancreatic cancer of Japan Pancreas Society.

construct was transiently transfected into scrambled control-siRNA and *BCL7B*-siRNA transfected S2-013 cells, and expression of myc-tagged BCL7B was confirmed (**Figure 5E**). The exogenous BCL7B from the rescue construct was localized in the cytoplasm of cell bodies and in cell protrusions of S2-013 cells, similar to endogenous BCL7B (**Figure 5F**).

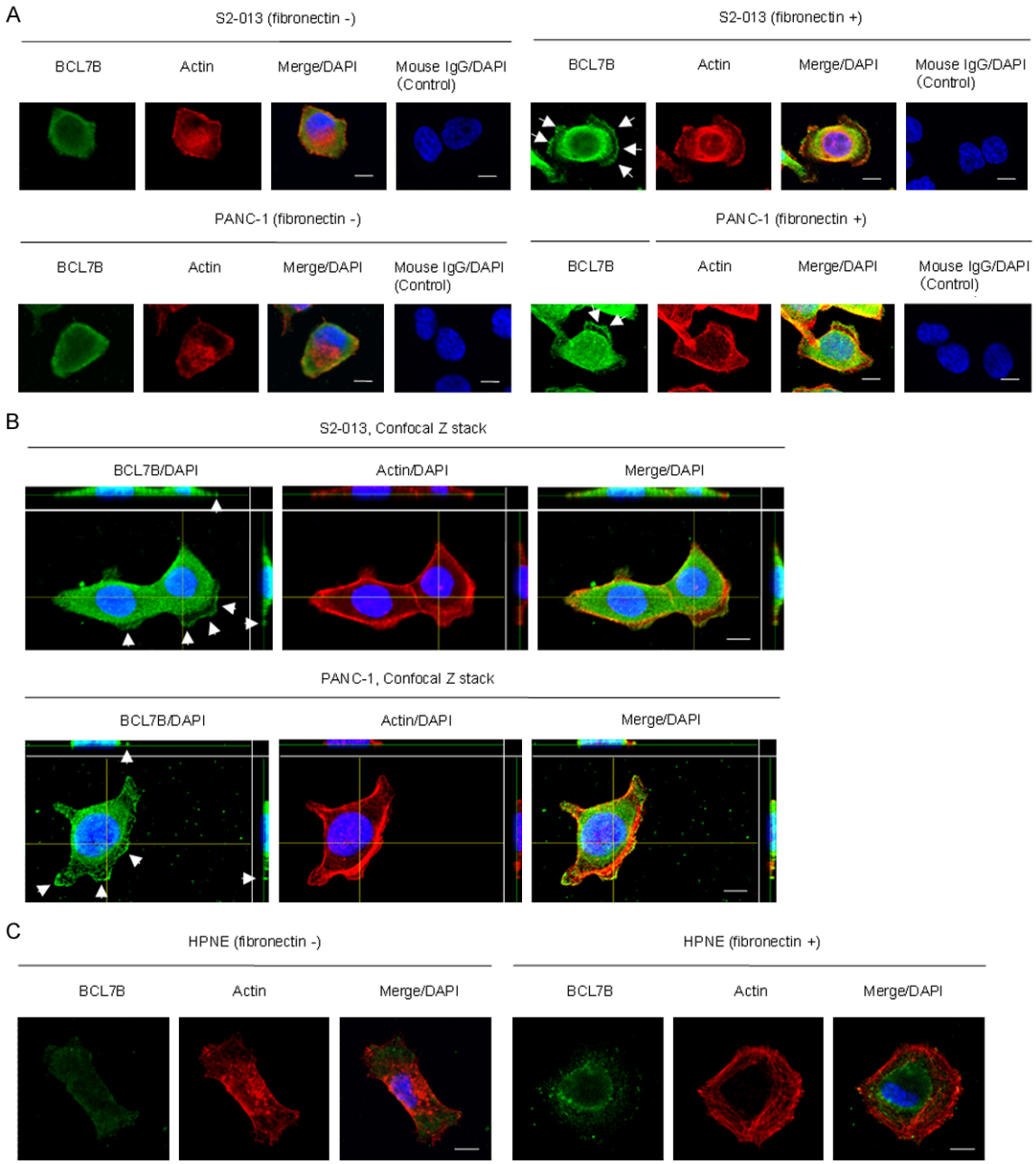

Figure 3. The distribution of BCL7B in PDAC cells. A. Immunocytochemistry on S2-013 and PANC-1 cells that were cultured with or without fibronectin. The cells were labeled with anti-BCL7B antibody (green) and phalloidin (red; actin filaments). Arrows; BCL7B localized in cell protrusions. Blue; DAPI staining. Scale bars; 10 μm. B. Confocal Z stack shows intracellular BCL7B and the accumulation of BCL7B (green) in membrane protrusions of S2-013 and PANC-1 cells grown on fibronectin. Actin filaments were labeled by phalloidin (red). Arrows; BCL7B localized in cell protrusions. The upper and right panels in the confocal Z stack show a vertical cross-section (yellow lines) through the cells. Scale bars; 10 μm. C. Immunocytochemistry on HPNE cells that were cultured with or without fibronectin. The cells were labeled with anti-BCL7B antibody (green) and phalloidin (red). Scale bars; 10 μm.

BCL7B-siRNA transfected S2-013 and PANC-1 cells expressing the rescue construct could rescue cell motility and invasiveness inhibited after BCL7B silencing (**Figure 5G** and **5H**). These results indicated that BCL7B promoted PDAC cell motility and invasion.

Roles of BCL7B in forming cell protrusions

We analyzed peripheral actin structures in membrane ruffles of scrambled control-siRNA and *BCL7B*-siRNA transfected S2-013 and PANC-1 cells cultured on fibronectin. Peripheral

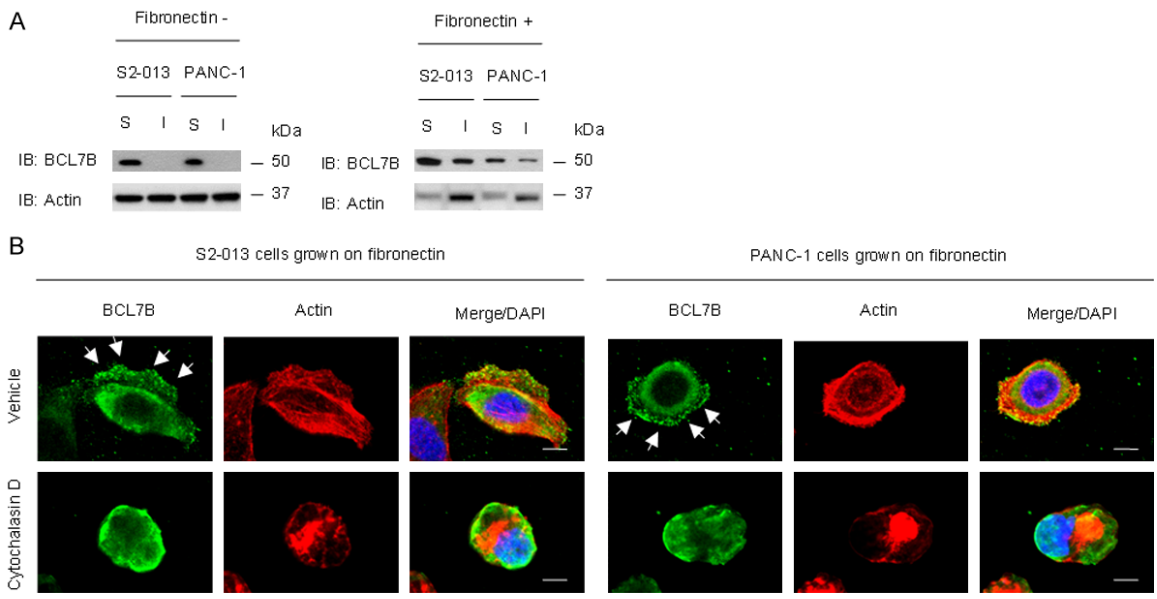

Figure 4. Association of subcellular localization of BCL7B with peripheral actin rearrangements. A. Cell lysates of S2-013 and PANC-1 cells cultured with or without fibronectin were fractionated into Triton X-100-soluble (S) and -insoluble (I) fractions. Each fraction was run on SDS-PAGE and blotted using anti-BCL7B and the JLA20 anti-actin antibodies. Data are representative of three independent experiments. B. Confocal immunofluorescence microscopic images of S2-013 and PANC-1 cells that were pretreated with 100 μM Cytochalasin D for 12 h and were then incubated on fibronectin. Cells were stained with anti-BCL7B antibody (green). Actin filaments were labeled with phalloidin (red). Arrows; BCL7B localized in cell protrusions. Blue; DAPI staining. Scale bars, 10 μm.

actin structures in cell protrusions were less abundant in *BCL7B*-siRNA transfected S2-013 and PANC-1 cells compared with control-siRNA transfected S2-013 and PANC-1 cells (S2-013, **Figure 6A**; PANC-1, **Figure 6B**). Next we tested whether the phenotypic effect of knockdown of BCL7B could be rescued by overexpression of BCL7B (S2-013, **Figure 6C**; PANC-1, **Figure 6D**). Transfection of a BCL7B-rescue construct into *BCL7B*-siRNA transfected S2-013 and PANC-1 cells rescued the decrease in peripheral actin structures at the protrusions caused by the *BCL7B*-siRNA.

To quantify the degree of inhibition caused by suppression of BCL7B, we observed the induction of membrane protrusions. In *BCL7B*-siRNA transfected S2-013 and PANC-1 cells cultured on fibronectin, suppression of BCL7B inhibited the formation of protrusions compared with control-siRNA transfected S2-013 and PANC-1 cells (S2-013, **Figure 7A**; PANC-1, **Figure 7B**). Transfection of a BCL7B-rescue construct into *BCL7B*-siRNA transfected S2-013 and PANC-1 cells rescued the decrease in the protrusions caused by the *BCL7B*-siRNA (S2-013, **Figure 7A**; PANC-1, **Figure 7B**). These results indicated that BCL7B drove rearrangement of peripheral actin to induce formation of additional membrane protrusions.

Links of BCL7B to associated cell signaling pathways

To determine whether BCL7B could regulate the activity of phosphoproteins, we performed phosphoprotein array analysis in the scrambled control-siRNA transfected S2-013 cells and *BCL7B*-siRNA transfected S2-013 cells grown on fibronectin (**Figure 8**). Of the 38 kinases investigated, suppression of BCL7B upregulated the activity of cAMP responsive element binding protein (CREB). Other kinases, including Src-family tyrosine kinases, did not show differences in phosphorylation between the scrambled control-siRNA transfected S2-013 cells and *BCL7B*-siRNA transfected S2-013 cells.

Effects of CREB on cell protrusion formation

CREB belongs to a large family of basic leucine zipper-containing transcription factors, including c-jun, c-fos and c-myc [6]. Although primarily localized in the nucleus, CREB can also be

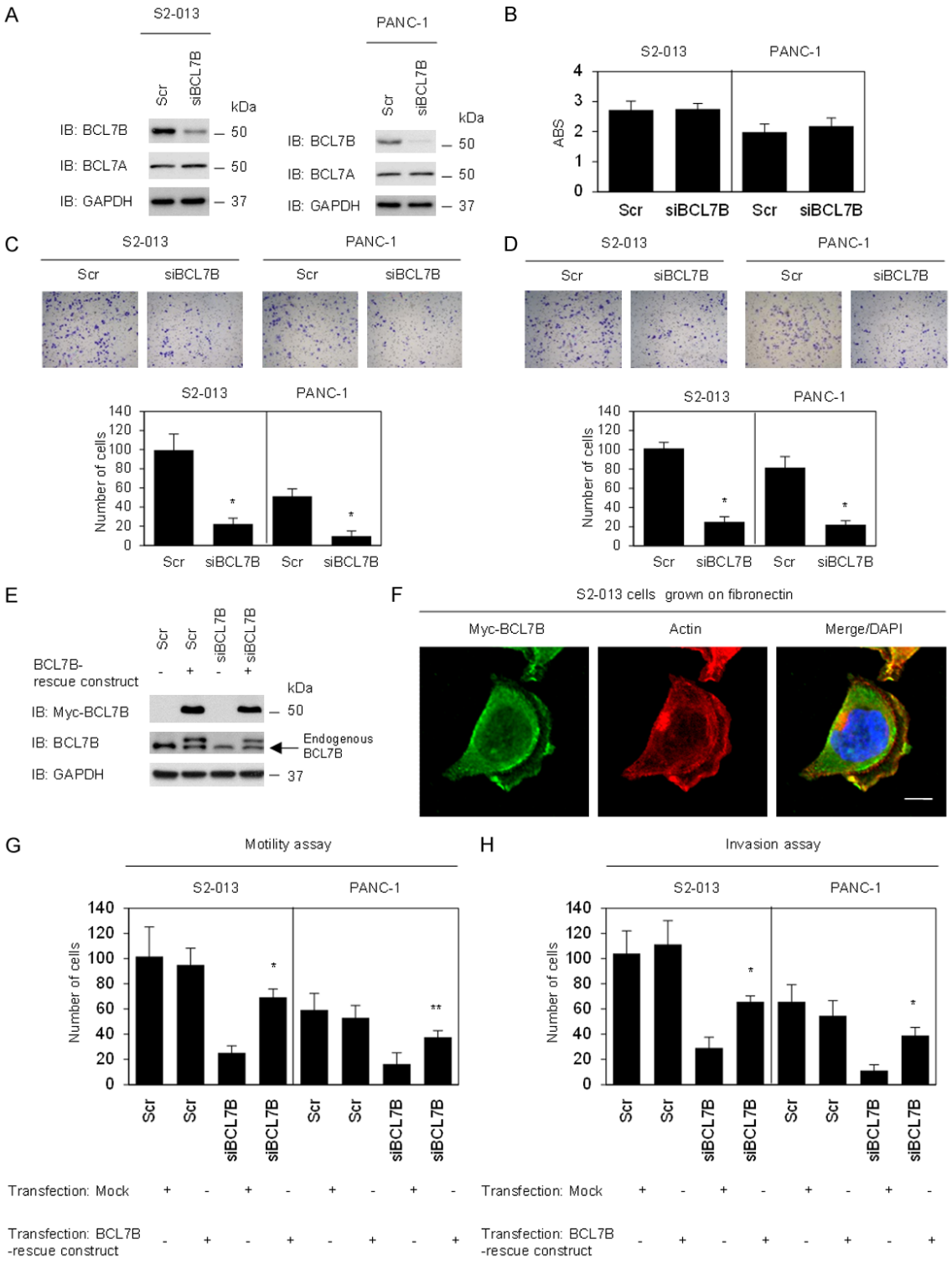

Figure 5. Roles of BCL7B in the motility and invasiveness of PDAC cells. (A) siRNA oligonucleotides targeting *BCL7B* (siBCL7B) or negative control scrambled siRNAs (Scr) were transiently transfected into S2-013 and PANC-1 cells. Western blotting was performed using anti-BCL7A and BCL7B antibodies. (B) Effects of knockdown of BCL7B on cell growth. S2-013 and PANC-1 cells were transiently transfected with Scr or siBCL7B for 48 h, and then MTT assay was used to measure cell growth. Data were derived from three independent experiments. *Columns*, mean; *bars*, SD. (C, D) Scr or siBCL7B was transiently transfected into S2-013 and PANC-1 cells. Motility (C) and two-chamber invasion assays (D) were performed. Migrating cells in four fields per group were scored. Data were derived from three independent experiments. *Columns*, mean; *bars*, SD. $*P < 0.005$ compared with Scr-transfected control (Stu-

dent's *t*-test). (E) Mock control vector or myc-tagged BCL7B-rescue construct were transiently transfected into Scr control-siRNA and *BCL7B*-siRNA transfected S2-013 cells. The endogenous and myc-tagged BCL7B was revealed by western blotting with anti-myc and anti-BCL7B antibodies. (F) S2-013 cells were transfected with a myc-tagged BCL7B-rescue construct, incubated on fibronectin and analyzed by confocal immunofluorescence, using anti-myc antibody (green). Actin filaments were labeled by phalloidin (red). Blue; DAPI staining. Scale bar; 10 μm. (G, H) Mock control vector or myc-tagged BCL7B-rescue constructs were transiently transfected into Scr control-siRNA and *BCL7B*-siRNA transfected S2-013 and PANC-1 cells, and 48 h later motility (G) and two-chamber invasion (H) assays were performed. Migrating cells in four fields per group were counted. Data were derived from three independent experiments. *Columns*, mean; *bars*, SD. $*P < 0.008$ and $**P < 0.05$ compared with corresponding *BCL7B*-siRNA transfected cells that were transfected with mock vector (Student's *t*-test).

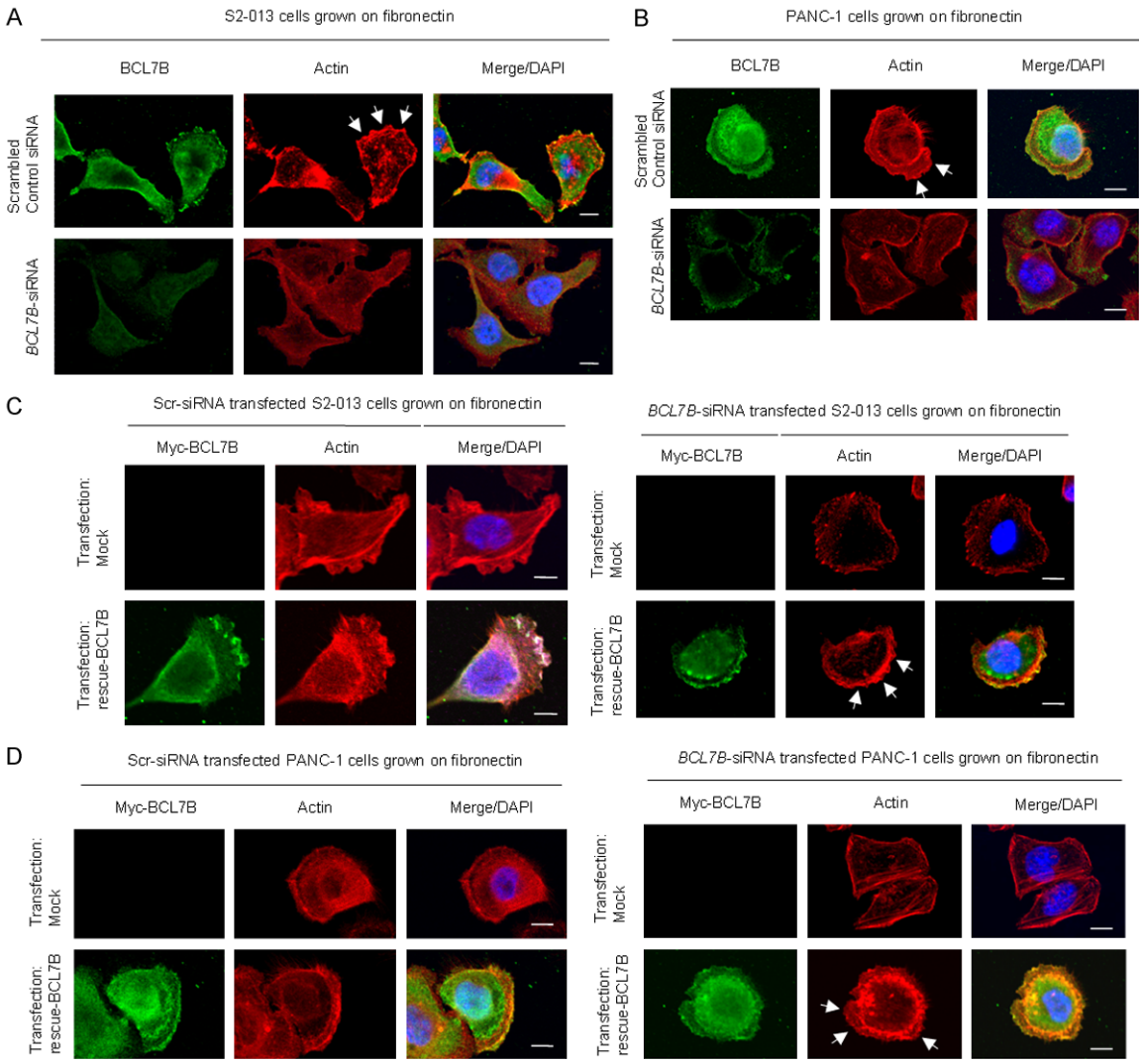

Figure 6. Roles of BCL7B in the peripheral actin rearrangements. (A, B) Confocal immunofluorescence microscopic images. siRNAs targeting *BCL7B* (siBCL7B) or negative control scrambled siRNAs (Scr) were transiently transfected into S2-013 (A) and PANC-1 (B) cells. The cells were incubated on fibronectin and screened with anti-BCL7B antibody (green) and phalloidin (red). Arrows; peripheral actin structures in cell protrusions of Scr-transfected cells. Blue; DAPI staining. Scale bars; 10 μm. (C, D) Confocal immunofluorescence microscopic images. The mock control vector or myc-tagged BCL7B-rescue construct were transiently transfected into Scr control-siRNA and *BCL7B*-siRNA transfected S2-013 (C) and PANC-1 (D) cells. 48 h later, the cells were incubated on fibronectin. Cells were stained with anti-myc antibody (green). Actin filaments were labeled by phalloidin (red). Arrows, cell protrusions reinstated by exogenous BCL7B in *BCL7B*-siRNA transfected cells. Blue; DAPI staining. Scale bars; 10 μm.

found in the cytoplasm and mitochondria [26]. Consistent with this, CREB was mainly localized in the nucleus of S2-013 and PANC-1 cells grown on fibronectin (**Figure 9A**). Suppression

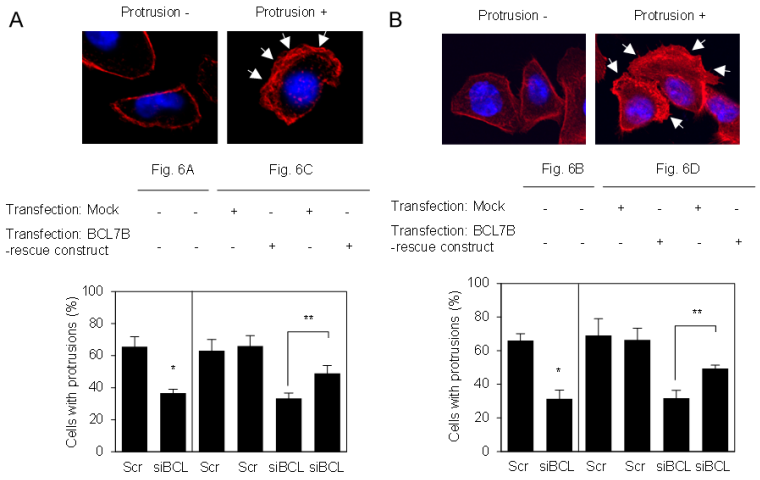

Figure 7. Quantification of the frequency of formation of actin-rich protrusions. (A, B) Quantification of the data shown in **Figure 6A** and **6C** (A), **Figure 6B** and **6D** (B). The values represent the number of cells with fibronectin-stimulated cell protrusions in which peripheral actin structures were increased. All cells in four fields per group were scored. Data were derived from three independent experiments. *Columns*, mean; *bars*, SD. *$P < 0.005$ compared with Scr-transfected control, and **$P < 0.05$ compared with *BCL7B*-siRNA transfected S2-013 cells that were subsequently transfected with mock vector (Student's *t*-test). Arrows; membrane protrusions that had many peripheral actin structures.

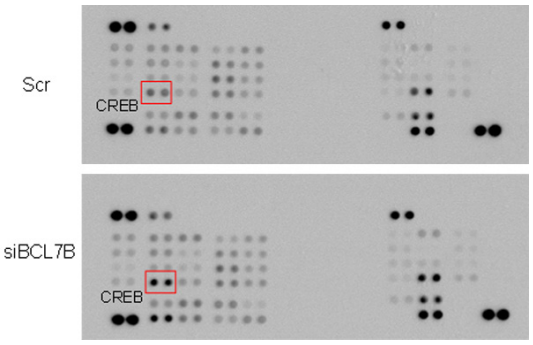

Figure 8. Analysis of cell signaling pathways that might associate with BCL7B activities. Human phosphoprotein arrays showing differential phosphorylation of proteins in scrambled control-siRNA transfected S2-013 cells and *BCL7B*-siRNA transfected S2-013 cells grown on fibronectin. Data are representative of three independent experiments.

of BCL7B did not significantly alter the subcellular localization of CREB in the nucleus of S2-013 and PANC-1 cells grown on fibronectin (S2-013, **Figure 9B** and **9D**; PANC-1, **Figure 9C** and **9D**).

To determine whether CREB participated in the induction of membrane protrusions, we analyzed peripheral actin structures in membrane ruffles of scrambled control-siRNA and *CREB*-siRNA transfected S2-013 and PANC-1 cells cultured on fibronectin. CREB expression in S2-013 and PANC-1 cells was transiently suppressed by *CREB*-specific siRNA (**Figure 10A**). Peripheral actin structures in cell protrusions were more abundant in *CREB*-siRNA transfected S2-013 and PANC-1 cells compared with control-siRNA transfected S2-013 and PANC-1 cells (S2-013, **Figure 10B**; PANC-1, **Figure 10C**). In *CREB*-siRNA transfected S2-013 and PANC-1 cells cultured on fibronectin, the formation of protrusions was induced compared with control-siRNA transfected S2-013 and PANC-1 cells (**Figure 10D**). These results indicated that CREB could decrease the formation of cell protrusions.

Roles of CREB in cell motility and invasion of PDAC cells

To determine whether CREB was involved in the motility and invasiveness of PDAC cells, CREB expression in S2-013 and PANC-1 cells was transiently suppressed by *CREB*-specific siRNA. In trans-well motility assays, the motility of S2-013 and PANC-1 cells was significantly higher in *CREB*-knockdown cells compared with control cells (**Figure 11A**). Cellular invasive potential was similarly assayed using Matrigel-coated Boyden chambers, and cell invasion was significantly promoted by silencing of CREB in S2-013 and PANC-1 cells (**Figure 11B**). A CREB-rescue construct was transiently transfected into S2-013 cells, and expression of myc-tagged CREB was confirmed in S2-013 cells (**Figure 11C**). The exogenous CREB from the rescue construct was localized in the nucleus and the cytoplasm of cell bodies in S2-013 cells grown on fibronectin (**Figure 11D**), similar to endogenous CREB. *CREB*-siRNA transfected S2-013 and PANC-1 cells expressing the rescue construct could abrogated the changes to cell motility and invasiveness that were caused by the *CREB*-siRNA (**Figure 11E** and **11F**). These results indicated that CREB inhibited the motility and invasiveness of PDAC cells.

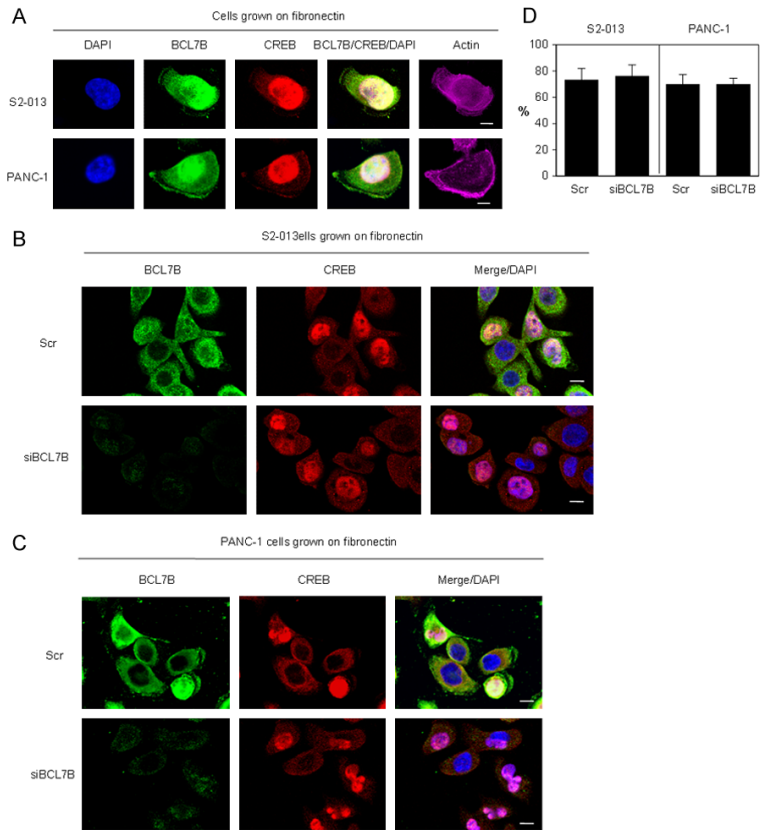

Figure 9. The distribution of CREB in PDAC cells. (A) Confocal immunofluorescence microscopic images. S2-013 and PANC-1 cells were cultured on fibronectin and then labeled with anti-BCL7B (green) and anti-CREB (red) antibody. Actin filaments were labeled by phalloidin (violet). Blue; DAPI staining. Scale bar; 10 μm. (B, C) Confocal immunofluorescence microscopic images. siRNAs targeting *BCL7B* (siBCL7B) or negative control scrambled siRNAs (Scr) were transiently transfected into S2-013 (B) and PANC-1 (C) cells. The cells were incubated on fibronectin and screened with anti-BCL7B antibody (green), anti-CREB antibody (red) and phalloidin (violet). Blue; DAPI staining. Scale bars; 10 μm. (D) Quantification of the nuclear localization of CREB in the confocal immunofluorescence microscopic images shown in (B and C) Data were derived from three independent experiments. *Columns*, mean; *bars*, SD.

Roles of BCL7B and CREB in cell motility and invasion of PDAC cells

To evaluate whether CREB is necessary for BCL7B to promote cell motility and invasion, we performed motility and two-chamber invasion assays in S2-013 and PANC-1 cells in which both BCL7B and CREB had been suppressed. Suppression of both BCL7B and CREB in S2-013 and PANC-1 cells did not significantly affect cell motility or invasion compared with control-siRNA transfected S2-013 and PANC-1 cells (**Figure 12A** and **12B**). We tested whether the phenotypic effect of knockdown of BCL7B could be rescued by overexpression of BCL7B in S2-013 and PANC-1 cells in which both BCL7B and CREB had been suppressed (**Figure 12A** and **12B**). Transfection of a BCL7B-rescue construct into S2-013 and PANC-1 cells in which both BCL7B and CREB had been suppressed did not rescue the decrease in cell motility and invasiveness caused by the *BCL7B*-siRNA. These results indicated that CREB was necessary for the BCL7B-associated promotion of motility and invasiveness.

Discussion

Our study revealed several new characteristics and functions of BCL7B: 1) overexpression of BCL7B in pancreatic cancer tissue was significantly correlated with overall survival, 2) BCL7B was accumulated in cell protrusions, and increased the formation of the protrusions, 3) BCL7B was associated with dephosphorylation of CREB, 4) CREB functioned in decreasing the formation of protrusions and inhibiting cell motility and invasion of PDAC cells, and 5) inhibition of CREB contributed to BCL7B-associated promotion of the motility and invasiveness of PDAC cells.

PDAC is known for its aggressive growth, and is characterized by early tissue invasion and metastasis with poor prognosis [27, 28]; however, BCL7B expression was not significantly correlated with any clinicopathologic factors. This may be due to the remarkably short overall survival of patients with PDAC. It is notable that patients with high BCL7B expression had significantly worse overall survival in both univariate and multivariate analyses, suggesting that it might be a novel and independent prognostic factor for PDAC. Moreover, we confirmed that BCL7B was not expressed in normal organs such as pancreas, brain, lung, liver, and kidney. Our results indicate that BCL7B is a significant

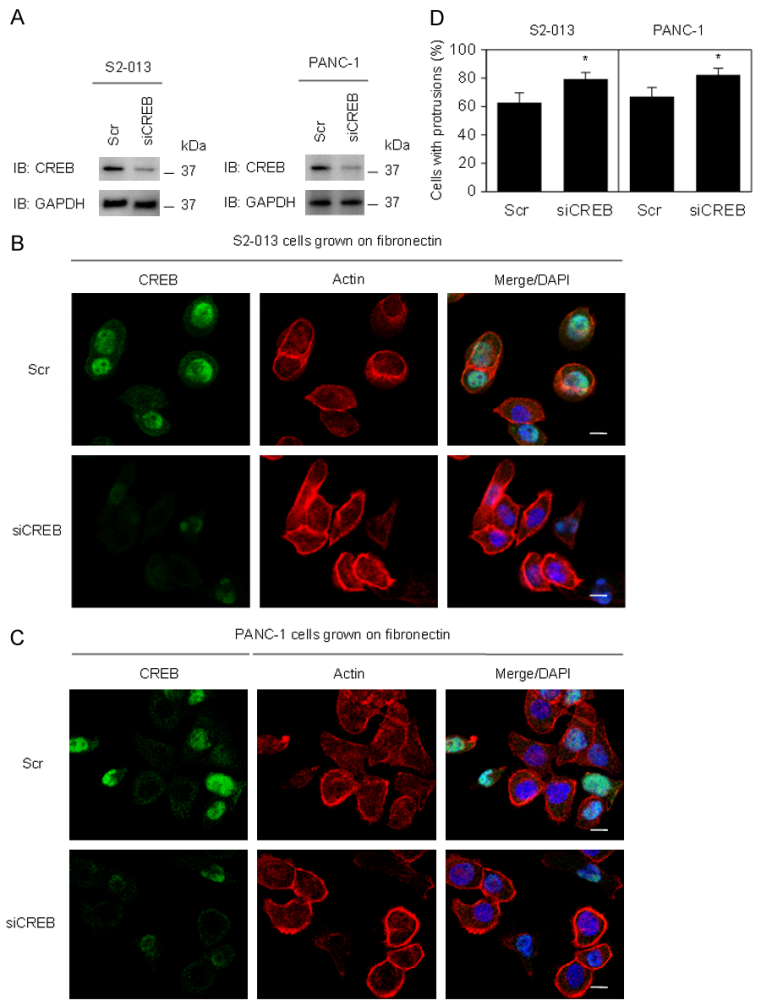

Figure 10. Roles of CREB in forming cell protrusions. (A) siRNA oligonucleotides targeting *CREB* (siCREB) or negative control negative control scrambled siRNAs (Scr) were transiently transfected into S2-013 and PANC-1 cells. Western blotting was performed using anti-CREB antibody. (B, C) Confocal immunofluorescence microscopic images. Scr or siCREB were transiently transfected into S2-013 (B) and PANC-1 (C) cells. The cells were incubated on fibronectin and screened with anti-CREB antibody (green) and phalloidin (red). Blue; DAPI staining. Scale bars; 10 μm. (D) Quantification of the data shown in (B and C). The values represent the number of cells with cell protrusions in which peripheral actin structures were increased. All cells in four fields per group were scored. Data were derived from three independent experiments. *Columns*, mean; *bars*, SD. **P* < 0.05 compared with the corresponding Scr-transfected control S2-013 and PANC-1 cells (Student's *t*-test).

prognostic factor that predicts the overall survival of patients with PDAC.

BCL7B is located in a chromosomal region commonly deleted in Williams syndrome [4]. The role of BCL7B loss in this syndrome is yet to be established. Furthermore, little is known about the roles of BCL7B in malignancies. We recently reported that insulin-like growth factor-2 mRNA-binding protein 3 (IGF2BP3) and IGF2BP3-bound mRNAs are localized in cytoplasmic RNA granules that accumulate in membrane protrusions of PDAC cells [29, 30]. IGF2BP3-bound mRNAs are preferentially translated in membrane protrusions inducing further formation of membrane protrusions, and promoting cell invasiveness and tumor metastasis [29, 30]. *BCL7B* mRNA is one of the IGF2BP3-bound transcripts in S2-013 cells grown on fibronectin [29]. Thus, our previous reports suggest that local translation of *BCL7B* mRNA in the protrusions may be associated with cell invasion and metastasis.

We showed that BCL7B was involved in the inactivation of CREB in PDAC cells. CREB is a crucial zinc finger transcriptional factor, which regulates a wide range of biological processes to orchestrate proper cell differentiation and cell growth [6, 7]. Zinc transport and zinc homeostasis play important roles in cancer progression, especially in PDAC and breast cancer [31, 32]. However, other reports have shown that CREB suppresses tumorigenesis, particularly by inhibiting the invasion and migration of PDAC, breast cancer and colorectal cancer cells [33, 34]. Similar to a previous report [33], we showed that knockdown of CREB increased cell protrusions and promoted cell motility and invasion of PDAC cells. The CREB pathway contributes to inhibiting the motility and invasiveness of PDAC cells by modulating the formation of cell protrusions. Knocking down both BCL7B and CREB did not modulate cell motility and invasion in PDAC cells, and the rescued expression of BCL7B did not promote cell motility and invasion in BCL7B-siRNA and CREB-siRNA transfected PDAC cells. These results indicated that CREB could play a critical role in BCL7B-

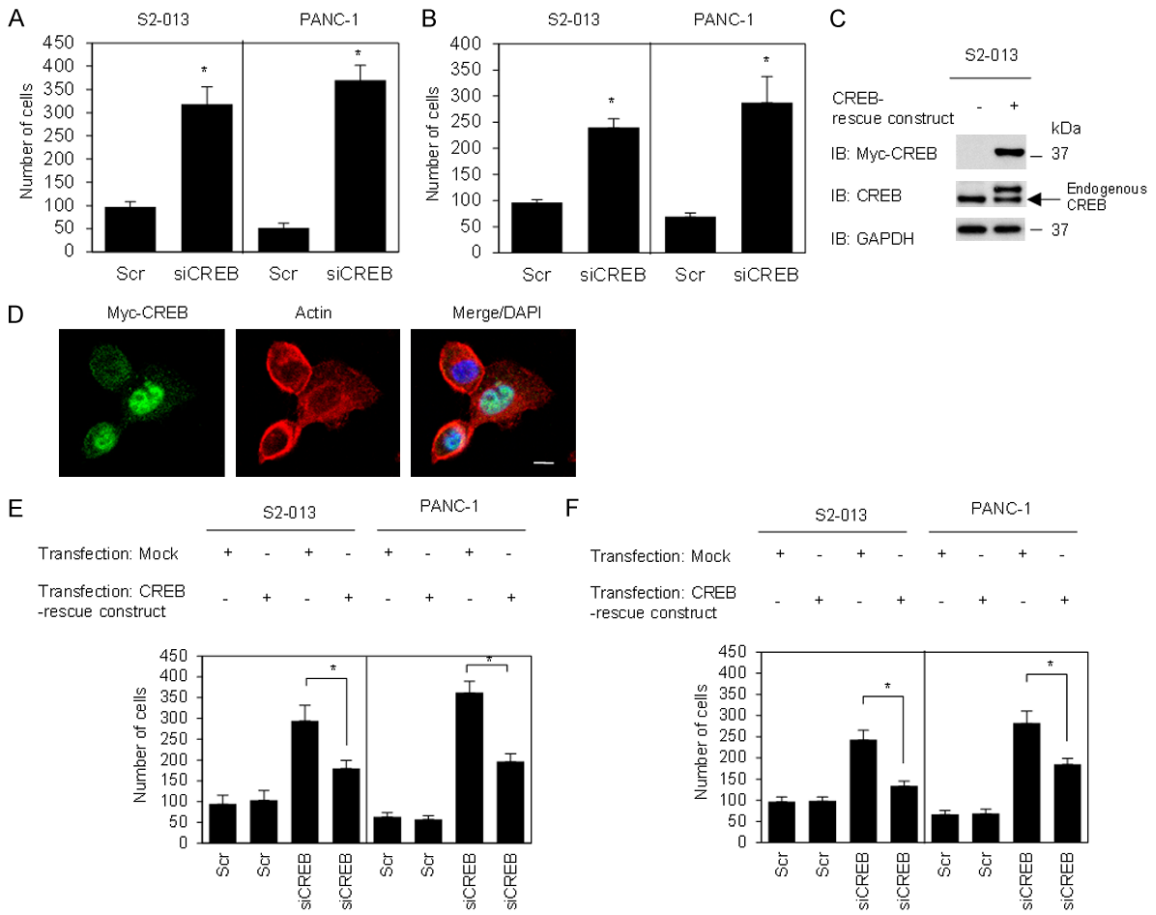

Figure 11. Roles of CREB in the motility and invasiveness of PDAC cells. (A, B) siRNA oligonucleotides targeting *CREB* (siCREB) or negative control scrambled siRNAs (Scr) were transiently transfected into S2-013 and PANC-1 cells. After 48 h, motility (A) and two-chamber invasion (B) assays were performed. Migrating cells in four fields per group were scored. Data are representative of three independent experiments. *Columns*, mean; *bars*, SD. **P* < 0.05 compared with Scr-transfected control (Student's *t*-test). (C) Mock control vector or myc-tagged CREB-rescue construct were transiently transfected into S2-013 cells. Western blotting was performed using anti-myc and anti-CREB antibodies. (D) S2-013 cells were transiently transfected with mock control vector or myc-tagged CREB-rescue construct, incubated on fibronectin and analyzed by confocal immunofluorescence, using anti-myc antibody (green). Actin filaments were labeled by phalloidin (red). Blue; DAPI staining. Scale bar; 10 μm. (E, F) Mock control vector or myc-tagged CREB-rescue constructs were transiently transfected into Scr control-siRNA and *CREB*-siRNA transfected S2-013 and PANC-1 cells and 48 h later motility (E) and two-chamber invasion (F) assays were performed. Migrating cells in four fields per group were counted. Data were derived from three independent experiments. *Columns*, mean; *bars*, SD. **P* < 0.02 compared with corresponding *CREB*-siRNA transfected cells that were transfected with mock vector (Student's *t*-test).

associated promotion of motility and invasiveness. The mechanisms by which BCL7B mediates the dephosphorylation of CREB, and CREB inhibits cell motility and invasion are still unknown. BCL7B-mediated dephosphorylation of CREB may contribute to the regulation of membrane ruffles, resulting in the promotion of PDAC cell motility and invasion. Future studies should evaluate BCL7B-associated CREB signaling cascades, and the transcriptional targets of CREB that coordinate the actin-cytoskeletal remodeling that is required for cell spreading and cell motility and invasion.

In conclusion, BCL7B promotes cell motility and invasion, and may be a useful marker for predicting the outcome of patients with PDAC. Mechanistically, we provide the first evidence that BCL7B-mediated dephosphorylation of CREB could regulate the formation of membrane protrusions, resulting in the promotion of PDAC cell motility and invasion. In addition, the

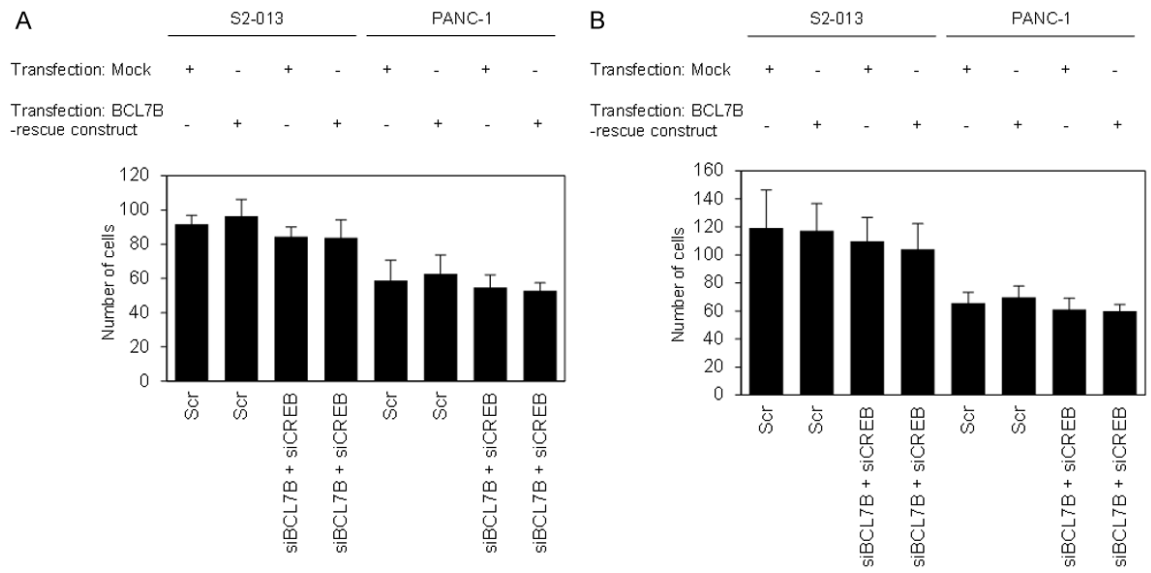

Figure 12. Association of BCL7B with CREB in cell motility and invasion. (A, B) A myc-tagged BCL7B-rescue construct was transfected into S2-013 and PANC-1 cells that had been transfected with *BCL7B*-siRNA and *CREB*-siRNA; 48 h later, motility (A) and two-chamber invasion (B) assays were performed. Migrating cells in four fields per group were counted. Data are derived from three independent experiments. *Columns*, mean; *bars*, SD.

functional importance of BCL7B mediated regulation of motility and invasiveness in PDAC cells suggests that inhibition of 1) BCL7B expression, 2) CREB dephosphorylation by BCL7B, or 4) a combination thereof, may be effective for PDAC targeted molecular therapy.

Acknowledgements

We thank Makiko Tsuboi, Miki Nishigawa, Rieko Takahashi and Shunichi Manabe for their excellent technical assistance. We thank Masahiko Sakaguchi for the statistical analysis of the data. This study was supported by a Grant-in-Aid for Scientific Research (KAKENHI) (245-91013, 15K14396, 17K09463).

Disclosure of conflict of interest

None.

Address correspondence to: Dr. Keisuke Taniuchi, Department of Endoscopic Diagnostics and Therapeutics, Kochi Medical School, Kochi University, Kohasu, Oko-cho, Nankoku, Kochi 783-8505, Japan. Tel: +81.88.880.2338; Fax: +81.88.880.2338; E-mail: ktaniuchi@kochi-u.ac.jp

References

[1] Zani VJ, Asou N, Jadayel D, Heward JM, Shipley J, Nacheva E, Takasuki K, Catovsky D and Dyer MJ. Molecular cloning of complex chromosomal translocation t(8;14;12)(q24.1;q32.3;q24.1) in a Burkitt lymphoma cell line defines a new gene (BCL7A) with homology to caldesmon. Blood 1996; 87: 3124-3134.

[2] Jadayel DM, Osborne LR, Coignet LJ, Zani VJ, Tsui LC, Scherer SW and Dyer MJ. The BCL7 gene family: deletion of BCL7B in Williams syndrome. Gene 1998; 224: 35-44.

[3] Pérez Jurado LA, Peoples R, Kaplan P, Hamel BC and Francke U. Molecular definition of the chromosome 7 deletion in Williams syndrome and parent-of-origin effects on growth. Am J Hum Genet 1996; 59: 781-792.

[4] Potter N, Karakoula A, Phipps KP, Harkness W, Hayward R, Thompson DN, Jacques TS, Harding B, Thomas DG, Palmer RW, Rees J, Darling J and Warr TJ. Genomic deletions correlate with underexpression of novel candidate genes at six loci in pediatric pilocytic astrocytoma. Neoplasia 2008; 10: 757-772.

[5] Zheng L, Foley K, Huang L, Leubner A, Mo G, Olino K, Edil BH, Mizuma M, Sharma R, and Le DT, Anders RA, Illei PB, Van Eyk JE, Maitra A, Laheru D and Jaffee EM. The tumor suppressor BCL7B functions in the wnt signaling pathway. PLoS Genet 2015; 11: e1004921.

[6] Mayr B and Montminy M. Transcriptional regulation by the phosphorylation-dependent factor CREB. Nat Rev Mol Cell Biol 2001; 2: 599-609.

[7] Shaywitz AJ and Greenberg ME. CREB: a stimulus-induced transcription factor activated by a

diverse array of extracellular signals. Annu Rev Biochem 1999; 68: 821-861.
[8] Abramovitch R, Tavor E, Jacob-Hirsch J, Zeira E, Amariglio N, Pappo O, Rechavi G, Galun E and Honigman A. A pivotal role of cyclic AMP-responsive element binding protein in tumor progression. Cancer Res 2004; 64: 1338-1346.
[9] Radhakrishnan I, Pérez-Alvarado GC, Parker D, Dyson HJ, Montminy MR and Wright PE. Solution structure of the KIX domain of CBP bound to the transactivation domain of CREB: a model for activator:coactivator interactions. Cell 1997; 91: 741-752.
[10] Thakur JK, Yadav A and Yadav G. Molecular recognition by the KIX domain and its role in gene regulation. Nucleic Acids Res 2014; 42: 2112-2125.
[11] Ruffell D, Mourkioti F, Gambardella A, Kirstetter P, Lopez RG, Rosenthal N and Nerlov C. A CREB-C/EBPbeta cascade induces M2 macrophage-specific gene expression and promotes muscle injury repair. Proc Natl Acad Sci U S A 2009; 106: 17475-17480.
[12] Strempel JM and Vercelli D. Functional dissection identifies a conserved noncoding sequence-1 core that mediates IL13 and IL4 transcriptional enhancement. J Biol Chem 2007; 282: 3738-3746.
[13] Zuloaga R, Fuentes EN, Molina A and Valdés JA. The cAMP response element binding protein (CREB) is activated by insulin-like growth factor-1 (IGF-1) and regulates myostatin gene expression in skeletal myoblast. Biochem Biophys Res Commun 2013; 440: 258-264.
[14] Hong SH, Goh SH, Lee SJ, Hwang JA, Lee J, Choi IJ, Seo H, Park JH, Suzuki H, Yamamoto E, Kim IH, Jeong JS, Ju MH, Lee DH and Lee YS. Upregulation of adenylate cyclase 3 (ADCY3) increases the tumorigenic potential of cells by activating the CREB pathway. Oncotarget 2013; 4: 1791-1803.
[15] Sakamoto KM and Frank DA. CREB in the pathophysiology of cancer: implications for targeting transcription factors for cancer therapy. Clin Cancer Res 2009; 15: 2583-2587.
[16] Tsuboi M, Taniuchi K, Furihata M, Naganuma S, Kimura M, Watanabe R, Shimizu T, Saito M, Dabanaka K, Hanazaki K and Saibara T. Vav3 is linked to poor prognosis of pancreatic cancers and promotes the motility and invasiveness of pancreatic cancer cells. Pancreatology 2016; 16: 905-916.
[17] Japan pancreatic society. Classification of pancreatic carcinoma. 2nd edition. Tokyo: Kanehara & Co; 2003.
[18] Sobin LH, Gospodarowicz MK and Witteknd C. TNM classification of malignant tumors. 7th edition. New York: Wiley-Blackwell 2009. pp. 132-135.
[19] Miyazawa Y, Uekita T, Hiraoka N, Fujii S, Kosuge T, Kanai Y, Nojima Y and Sakai R. CUB domain-containing protein 1, a prognostic factor for human pancreatic cancers, promotes cell migration and extracellular matrix degradation. Cancer Res 2010; 70: 5136-5146.
[20] Iwamura T, Katsuki T and Ide K. Establishment and characterization of a human pancreatic cancer cell line (SUIT-2) producing carcinoembryonic antigen and carbohydrate antigen 19-9. Jpn J Cancer Res 1987; 78: 54-62.
[21] Deer EL, González-Hernández J, Coursen JD, Shea JE, Ngatia J, Scaife CL, Firpo MA and Mulvihill SJ. Phenotype and genotype of pancreatic cancer cell lines. Pancreas 2010; 39: 425-435.
[22] Lee KM, Yasuda H, Hollingsworth MA and Ouellette MM. Notch2-positive progenitors with the intrinsic ability to give rise to pancreatic ductal cells. Lab Invest 2005; 85: 1003-1012.
[23] Taniuchi K, Nishimori I and Hollingsworth MA. Intracellular CD24 inhibits cell invasion by posttranscriptional regulation of BART through interaction with G3BP. Cancer Res 2011; 71: 895-905.
[24] Tanouchi A, Taniuchi K, Furihata M, Naganuma S, Dabanaka K, Kimura M, Watanabe R, Kohsaki T, Shimizu T, Saito M, Hanazaki K and Saibara T. CCDC88A, a prognostic factor for human pancreatic cancers, promotes the motility and invasiveness of pancreatic cancer cells. J Exp Clin Cancer Res 2016; 35: 190.
[25] Taniuchi K, Yokotani K and Saibara T. BART inhibits pancreatic cancer cell invasion by Rac1 inactivation through direct binding to active Rac1. Neoplasia 2012; 14: 440-450.
[26] Shibanuma M, Ishikawa F, Kobayashi M, Katayama K, Miyoshi H, Wakamatsu M, Mori K and Nose K. Critical roles of the cAMP-responsive element-binding proteinmediated pathway in disorganized epithelial phenotypes caused by mitochondrial dysfunction. Cancer Sci 2012; 103: 1803-1810.
[27] Baumgart M, Heinmöller E, Horstmann O, Becker H and Ghadimi BM. The genetic basis of sporadic pancreatic cancer. Cell Oncol 2005; 27: 3-13.
[28] Ahrendt SA and Pitt HA. Surgical management of pancreatic cancer. Oncology 2002; 16: 725-734.
[29] Taniuchi K, Furihata M, Hanazaki K, Saito M and Saibara T. IGF2BP3-mediated translation in cell protrusions promotes cell invasiveness and metastasis of pancreatic cancer. Oncotarget 2014; 5: 6832-6845.
[30] Taniuchi K, Furihata M and Saibara T. KIF20A-mediated RNA granule transport system promotes the invasiveness of pancreatic cancer cells. Neoplasia 2014; 16: 1082-1093.

[31] Li M, Zhang Y, Liu Z, Bharadwaj U, Wang H, Wang X, Zhang S, Liuzzi JP, Chang SM, Cousins RJ, Fisher WE, Brunicardi FC, Logsdon CD, Chen C and Yao Q. Aberrant expression of zinc transporter ZIP4 (SLC39A4) significantly contributes to human pancreatic cancer pathogenesis and progression. Proc Natl Acad Sci U S A 2007; 104: 18636-18641.

[32] Kagara N, Tanaka N, Noguchi S and Hirano T. Zinc and its transporter ZIP10 are involved in invasive behavior of breast cancer cells. Cancer Sci 2007; 98: 692-697.

[33] Zimmerman NP, Roy I, Hauser AD, Wilson JM, Williams CL and Dwinell MB. Cyclic AMP regulates the migration and invasion potential of human pancreatic cancer cells. Mol Carcinog 2015; 54: 203-215.

[34] Hansen C, Howlin J, Tengholm A, Dyachok O, Vogel WF, Nairn AC, Greengard P and Andersson T. Wnt-5a-induced phosphorylation of DARPP-32 inhibits breast cancer cell migration in a CREB-dependent manner. J Biol Chem 2009; 284: 27533-27543.